

# Spatial Interrelationships between Lake Elevations, Water Tables, and Sinkhole Occurrence in Central Florida: A GIS Approach

Dean Whitman, Timothy Gubbels, and Linda Powell

## Abstract

Sinkholes constitute the principal geologic hazard in central Florida. Local hydrogeology is recognized as an important factor in their formation. We use a GIS to investigate the spatial relationships between hydrogeology and sinkhole formation near Orlando, Florida. Landsat TM imagery, digital topography, and well data are used to construct a model of the head difference between a discontinuous set of surficial aquifers and the Floridan aquifer, a regionally extensive confined aquifer. This model is quantitatively compared to a buffer model of distance to nearest sinkhole constructed from a database of collapse events. Sinkhole occurrence is positively associated with regions where the head difference is between 5 and 15 m. In these regions, sinkholes are more common and more closely spaced than expected. In contrast, sinkholes are less frequent and farther apart than expected in regions of low head difference. This association of sinkhole proximity to high head difference demonstrates the importance of hydrostatic loads in sinkhole hazard.

## Introduction

Central Florida is well known for its numerous karst lakes and landforms. Sinkholes are ubiquitous features of karst terrains and constitute a major geologic hazard in central Florida. The term "sinkhole" refers to an area of localized land-surface subsidence, or collapse, due to karst processes, which results in a closed circular depressions of moderate dimensions (Monroe, 1970; Sweeting, 1973; White, 1988). Sinkholes are formed by the subsidence or collapse of surficial material into subsurface cavities in regions underlain by limestone and other rocks susceptible to dissolution by ground water. They typically form funnel-shaped depressions ranging in size from meters to hundreds of meters. Although many sinkholes form by processes of progressive subsidence, formation by catastrophic collapse is common and, because of its inherent suddenness, is a major geologic hazard. Both sudden and progressive formation of sinkholes damages roads, bridges, power transmission lines, pipelines, buildings, and farmland, and results in massive financial losses to society. For example, a single collapse event, the Winter Park, Florida sinkhole of May 1981, caused over 4 million dollars in damages (Jammal, 1982). Between 1970 and 1980 sinkhole-related damages in the U.S. alone exceeded 200 million dollars (Newton, 1987), and global damages over the

past 25 years probably exceed 1 billion dollars, as sinkhole development affects approximately 15 percent of the world (Wilson and Beck, 1992).

Existing studies of sinkhole hazards have traditionally been the province of civil engineers, geologists, and hydrologists accustomed to working at local scales (e.g., Benson and La Fountain, 1984; Wilson and Beck, 1988). New remotely sensed data sets and computer-based techniques developed during the 80s and 90s have opened the opportunity for more synoptic study of the sinkhole hazard. The resolutions of commonly available satellite imagery — 30 m for Landsat TM and 10 m for SPOT — impose firm limits to the detection of small natural objects such as sinkholes, and this scale limitation prevents their use for direct local or regional mapping of sinkholes. Instead, these data sets offer potential for understanding sinkhole collapse hazard by permitting the direct synoptic spatial analysis of such related phenomena as topography, surface hydrology, and land use. Comparison of these data with an independently derived historical sinkhole occurrence database allows questions of sinkhole hazard to be addressed on a regional scale.

This study demonstrates the utility of computer visualization and geographic information system (GIS) software for investigating the triggering phenomena of geologic hazards. A GIS provides the ability to organize, visualize, and merge spatial datasets from different sources and allows quantitative spatial analysis and predictive modeling of these data. In this study, these tools are used to examine some of the regional geologic phenomena that influence the sinkhole hazard in central Florida. In particular, we examine the spatial interrelationships between hydrostatic heads of a surficial and a confined aquifer system and the locations of reported sinkholes in central Florida.

## Regional Setting

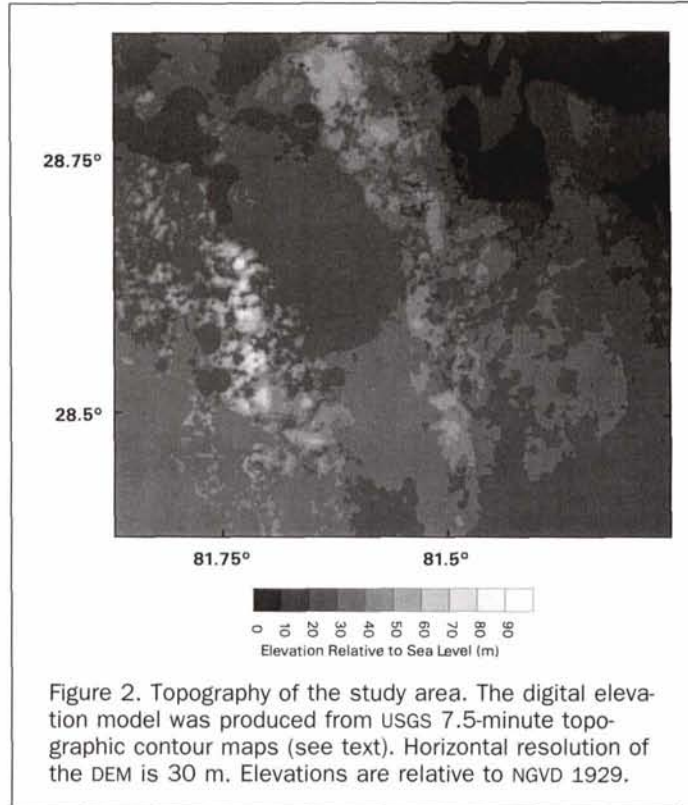
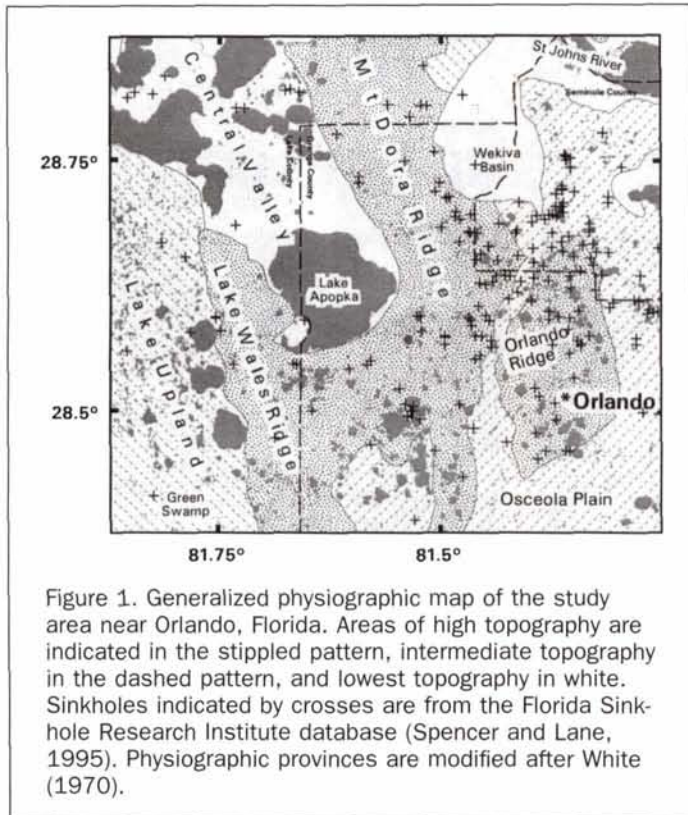
The study area lies adjacent to the rapidly growing Orlando metropolitan area and includes parts of Lake, Orange, and Seminole counties, covering approximately 3500 km<sup>2</sup>. The most distinct physiographic features are the sand covered Lake Wales, Mt. Dora, and Orlando ridges (Figure 1). These ridges are relict coastal features and correspond to the areas of greatest unconsolidated sediment thickness (Lichtler *et al.*,

D. Whitman and L. Powell are with Florida International University, Miami, Florida 33199 (whitmand@fiu.edu).

T. Gubbels is with Raytheon Systems, Landover, MD 20774.

Photogrammetric Engineering & Remote Sensing,  
Vol. 65, No. 10, October 1999, pp. 1169–1178.

0099-1112/99/6510-1169\$3.00/0  
© 1999 American Society for Photogrammetry  
and Remote Sensing



1968; White, 1970). Elevations range from 30 to 94 m (Figure 2). The topographic ridges serve to localize the first-order peninsular drainage divides and form the boundaries for the Saint Johns, Kissimmee, and Withlacoochee river drainage basins. The ridges are surrounded by the lower relief Lake Upland and Osceola Plain. The Central Valley lies between the sandy ridges and is occupied by several large shallow lakes, including Lake Apopka. The lowest elevations in the study area correspond to the Wekiva basin and St. Johns River valley.

Viewed from space, the most prominent surface feature of the study area are lakes (Figure 3). There are approximately 1500 discrete lakes in this region, the namesake for Lake County. These lakes cover over 600 km<sup>2</sup>, or 17 percent of the surface area. In places, groups of lakes are localized by and aligned along the sandy ridges (Figures 2 and 3). Most of these lakes occupy solution depressions. These solution depressions are distinct from recent sinkholes; they generally are much larger and have formed over much greater lengths of time (possibly up to millions of years). There is a general absence of surface drainage. Where streams are present, the drainage pattern is disorganized. Rather than form surface runoff, rainfall within this region infiltrates the subsurface. This area thus forms an important recharge region for the underlying aquifers (Lichtler *et al.*, 1968).

The Florida peninsula is underlain by an extensive system of aquifers contained in Cenozoic limestones and clastic sediments (Table 1). In the study area, three distinct hydrostratigraphic units exist: Floridan Aquifer, the Intermediate Confining Unit, and the Surficial Aquifer System (Florida Geological Survey, 1986; Miller, 1986; Miller, 1997). The Floridan is a regionally extensive aquifer system situated within a thick sequence of Paleocene to early Miocene age limestones which have been subjected to extensive dissolution and cavity formation. The Floridan aquifer provides the principle municipal and agricultural water supply for much of central

and northern Florida. Spatial and temporal variations in its potentiometric surface are often related to groundwater withdrawal.

In the study area, the Floridan aquifer is capped by Miocene age, variable thickness, low permeability clay rich clastic sediments of the Hawthorn group. This unit acts as an aquitard and forms the intermediate confining unit of the

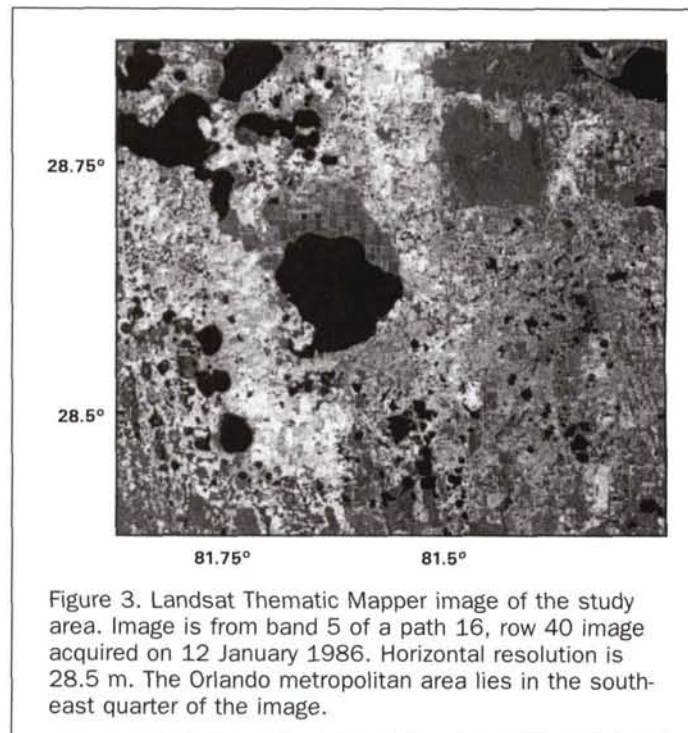


TABLE 1. GENERALIZED STRATAGRAPHIC AND HYDROGEOLOGIC UNITS, ORLANDO, FLORIDA REGION. STRATIGRAPHY IS FROM LICHTER *ET AL.* (1968) AND JOHNSON (1979). HYDROGEOLOGIC TERMINOLOGY FROM FLORIDA GEOLOGIC SURVEY (1986).

Series	Stratigraphic Unit	Thickness (m)	Hydrogeologic Unit	Lithology
Holocene Plio-Pleistocene	Alluvium and terrace deposits	0-50	Surficial Aquifer System	Undifferentiated quartz sand, and shell beds with some clay
Miocene	Hawthorn Group	3-50	Intermediate Confining Unit	Clayey sand and silt, phosphatic sand, some limestone
Eocene	Ocala Group	0-30	Upper Floridan Aquifer	Granular, porous limestone
	Avon Park Limestone	100-180		Some dolomitic limestone

Floridan aquifer. It varies in thickness from less than 15 m in the southwest and northeast corners of the study area to over 50 m beneath the southern Mt. Dora Ridge (Murray and Halford, 1996). The Hawthorn is covered by variable thickness, permeable, undifferentiated sand, silt, and shell beds which range in age from Pliocene to Holocene. These units are generally thickest beneath the topographic ridges and form a set of unconfined, discontinuous aquifers known as the surficial aquifer system. Because of its general low productivity and poor water quality, this aquifer system is rarely used for potable water supplies and, in contrast to the Floridan, the water tables of these surficial aquifers are more directly influenced by changes in rainfall, runoff, and land use.

Because large areas of the state are underlain at relatively shallow depths by carbonate bedrock, sinkholes are widespread in Florida (Schmidt and Scott, 1984; Upchurch and Randazzo, 1997). During the 1980s, the Florida Sinkhole Research Institute (FSRI) at the University of Central Florida compiled an excellent computerized inventory of new sinkhole occurrence in the state of Florida (Wilson and Beck, 1992; Spencer and Lane, 1995; Wilson and Shock, 1996). This database contains over 1900 reported sinkholes occurring between 1960 and 1991 and includes information on location, date of occurrence, dimensions, and hydrogeologic setting for each sinkhole. The study area contains 226 reported sinkholes from the FSRI database (Figure 1). The majority of these sinkholes occur in the eastern half of the study area on or adjacent to the Mt. Dora and Orlando Ridges.

Most of the sinkholes within the study area form due to cover collapse (Sinclair and Stewart, 1985). Cover-collapse sinkholes occur where the limestone is covered by clay-rich (Hawthorn group) sediments with sufficient cohesion to bridge cavities in the limestone. These sinkholes occur abruptly when the cover collapses into the cavities and are typically the most hazardous type of sinkhole. A simplified developmental model of a cover-collapse sinkhole is shown in Figure 4. The sinkhole formation process begins with the formation of a solution cavity within limestone near the top of the Floridan aquifer. As this cavity grows upward, it is bridged by the cohesive Hawthorn group sediments. Collapse occurs when the cohesive strength of the bridge becomes insufficient to support the weight of the overlying material. The clastic materials of the cover unit fail and flow downward into the cavity. As a result, a steep-sided surface depression forms.

The local hydrogeology plays an important role in triggering or retarding cover-collapse sinkholes. Water in the surficial aquifer system acts as a load, causing a downward hydrostatic force on the roof of the cavity. In contrast, water pressure within the Floridan aquifer provides an upward force supporting the cavity roof. Thus, a large positive head difference between the surficial and the Floridan aquifer systems can be a major driving factor in sinkhole collapse. Specific triggering mechanisms include drops in the level of the Floridan potentiometric surface, caused by excessive well withdrawals, and rises in the water table of the surficial aquifer.

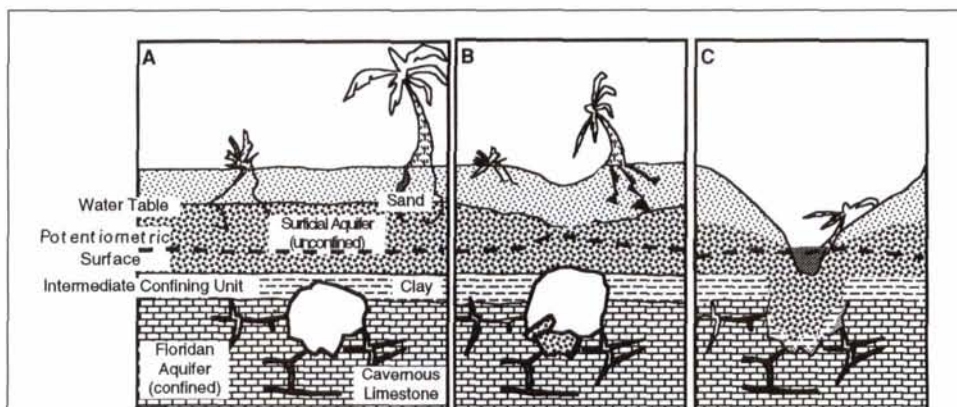


Figure 4. Model of cover collapse sinkhole formation. Cover collapse sinkholes generally occur in areas where unconsolidated semi-cohesive cover overlies a confining unit above limestone strata. **A:** The process is initiated by the formation of a large cavity within the Limestone unit. **B:** As this cavity expands upward into the confining unit (Hawthorn). **C:** Collapse occurs when the cohesive strength of the roof is exceeded by vertical stress due to the weight of the overlying material. When the water table of the surficial aquifer lies above the potentiometric surface of the confined Floridan aquifer, an additional downward load is applied to the roof of the cavity. Modified after Lane (1986).

uifer system, caused by increased precipitation or surface water impoundments (Sinclair, 1982; Metcalfe and Hall, 1984; Newton, 1984; Sinclair *et al.*, 1985; Sinclair and Stewart, 1985; Wilson and Beck, 1992).

## Construction of Aquifer Models

### Approach

As mentioned above, numerous studies suggest that the hydrostatic head difference between the surficial and Floridan aquifers plays an important role in sinkhole occurrence. For an unconfined aquifer, such as the surficial aquifer, the "hydrostatic head" is defined as the altitude of the water table. For a confined aquifer, such as the Floridan, the hydrostatic head is defined as the level to which water rises in tightly cased wells penetrating the aquifer, and is represented physically by the "potentiometric surface" (Figure 4.) In order to explore the relationships between hydrostatic heads and sinkhole occurrence, a model of "head difference" between these aquifer systems needs to be constructed. This model is then compared both qualitatively and quantitatively to the locations of reported sinkholes.

The processing flow is shown in Figure 5. The analysis starts with three basic data sources: topography, Landsat imagery, and well data. First, satellite imagery and a digital elevation model are used to derive a map of lake surface elevations. This map is used as a model of the water table of the surficial aquifer system. Then, well data are used to construct a gridded representation of the Floridan aquifer potentiometric surface. The potentiometric surface grid is then subtracted from the lake elevation map to produce a map of lake elevations relative to the Floridan aquifer potentiometric surface. Finally, a head difference model is constructed and compared with a sinkhole database.

### Surficial Aquifer Model

In the study area, the water table generally lies above the potentiometric surface of the Floridan aquifer (Lichtler *et al.*, 1968; Boniol *et al.*, 1993; this study). Because the surficial aquifer system is not used for municipal and agricultural water supplies, relatively few monitoring wells sample it and precise maps of the water table generally do not exist. Because their surfaces intersect the water table locally, lakes provide a convenient surrogate means of mapping lateral variations in water table elevation, especially in areas where they are numerous. In this study, water surface elevations of the numerous lakes in the study area are used as a model of the head of the surficial aquifer system.

Satellite imagery and a digital elevation model (Figures 3 and 2) are used to determine the locations and elevations of surface water bodies. First, a 30-m horizontal resolution digital elevation model (DEM) is constructed for the study area (Figure 2). This DEM is produced from 5-foot-interval topographic contours and water body shorelines digitized from 20 separate USGS 7.5-minute quadrangle maps. The contour and shoreline vectors are used to construct a triangulated irregular network (TIN) surface model. Elevation values on a regularly spaced grid, with a grid spacing interval of 30 m, are calculated from the TIN by linear interpolation. This DEM is as good as, or of higher quality than, the comparable 7.5-minute USGS DEMs which are available in only limited areas in the study area.

Next, a binary raster mask of surface water bodies is extracted from a geocoded Landsat Thematic Mapper image acquired in January 1986. To do this, a band ratio image is computed by dividing band 2 by band 5. Because of the low reflectance of surface water in the middle infrared wavelengths, this 2/5 ratio is an extremely robust way of extracting water from Landsat imagery. The ratio image is constructed using a threshold value of 1.0. In the resultant surface water body image mask, water is assigned a value of 1 and land a value of null.

The water body mask is resampled to the DEM resolution and digitally overlaid on the DEM. The elevation of each water body pixel is assigned the corresponding DEM pixel elevation. The resulting raster map of lake elevations is shown in Plate 1A. In general, lake elevations decrease in a northeasterly direction from around 35 m above sea level in the Green Swamp area to near sea level in the St. Johns River.

The elevations of the lakes and the water table are not static. They change over time in response to seasonal and long term fluctuations in climate and water use. While the locations of the lakes are based on a contemporary data set, their elevations are based on quadrangle maps, most of which date back to the 1950s. More recent lake stage data are available for many of the larger lakes in central Florida (USGS, 1986a). Within the study area, however, stage records exist for less than 15 lakes, and this is inadequate for characterizing the complex spatial variations of the surficial aquifer system.

In order to quantify the temporal variation in lake surface elevations, we compared lake stage records within the study area for the Autumn of 1986 (USGS, 1986a) with lake elevations derived from the DEM. In all cases, the 1986 lake stage records are within 2 m of those on the quadrangle maps, with the vast majority within less than 1 m. This relatively small long term change in lake surface elevations suggests that the water table has been relatively unaffected by ground water development in the region since the 1950s (Murray and Halford, 1996). Short term fluctuations in lake levels are also affected by seasonal rainfall, but are in most cases small (Lichtler *et al.*, 1968; Lichtler *et al.*, 1976). For the purposes of this study, the lake elevation map is assumed to be representative of the long term average water table of the surficial aquifer system.

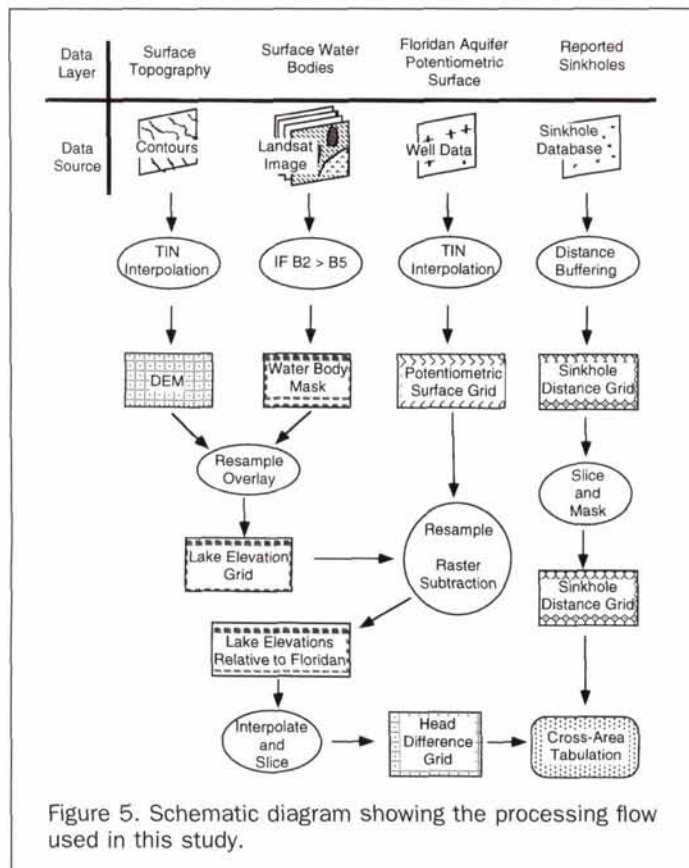


Figure 5. Schematic diagram showing the processing flow used in this study.

### Head Difference Model

The potentiometric surface for the Floridan aquifer is routinely measured in the field by the USGS and Florida state agencies using a widespread network of monitoring wells. Extensive ground-water development of the Floridan aquifer has led to a drawdown of the potentiometric surface of nearly 5 m in parts of the study area since 1950 (Miller, 1986; Murray and Halford, 1996). By the mid-1980s, this decline had decreased and the potentiometric surface was in quasi-steady-state conditions (Murray and Halford, 1996). For this study, well data from September 1985 (Schiner and Hays, 1985; USGS 1986b) and TIN interpolation are used to construct a potentiometric surface grid (Plate 1A). This time period was chosen to correspond to the satellite image used to map the lakes. In addition, this period roughly encloses the median occurrence date of the sinkholes from the FSRI database within the study area.

Contours of this surface are shown in Plate 1A. The surface generally dips to the northeast from around 35 m above sea level in the southwest part of the study area to less than 10 m in the northeast (Plate 1A). Raster subtraction of the potentiometric surface from the lake elevation map is used to produce a map of the lake elevations relative to the Floridan aquifer potentiometric surface (Plate 1B). This map is a first-order expression of the head difference between the Floridan and surficial aquifers.

The elevations of most lakes lie at or slightly above the elevation of the Floridan. This suggests that many of the lakes communicate with the Floridan aquifer by seepage through the intermediate confining (e.g., Lichtler *et al.*, 1976; Motz, 1998). A smaller but distinct population of lakes lies at elevations significantly above the Floridan potentiometric surface. These lakes tend to be concentrated in the eastern half of the study area on the Mount Dora and Orlando ridges (Compare Figure 1 and Plate 1). Somewhat surprisingly, lakes with surface elevations significantly above the Floridan potentiometric surface are absent from the Lake Wales Ridge. One notable exception to this pattern is a series of small water bodies located to the south of Lake Apopka on the Lake Wales Ridge, which have surfaces between 10 and 25 m above the Floridan potentiometric surface (Plate 1 and Figure 6). Field observations indicate that in all cases these water bodies correspond to hydraulic sand quarrying operations. Because these are not natural features of the landscape, we do not feel that they are representative of the general hydrogeologic setting of the region.

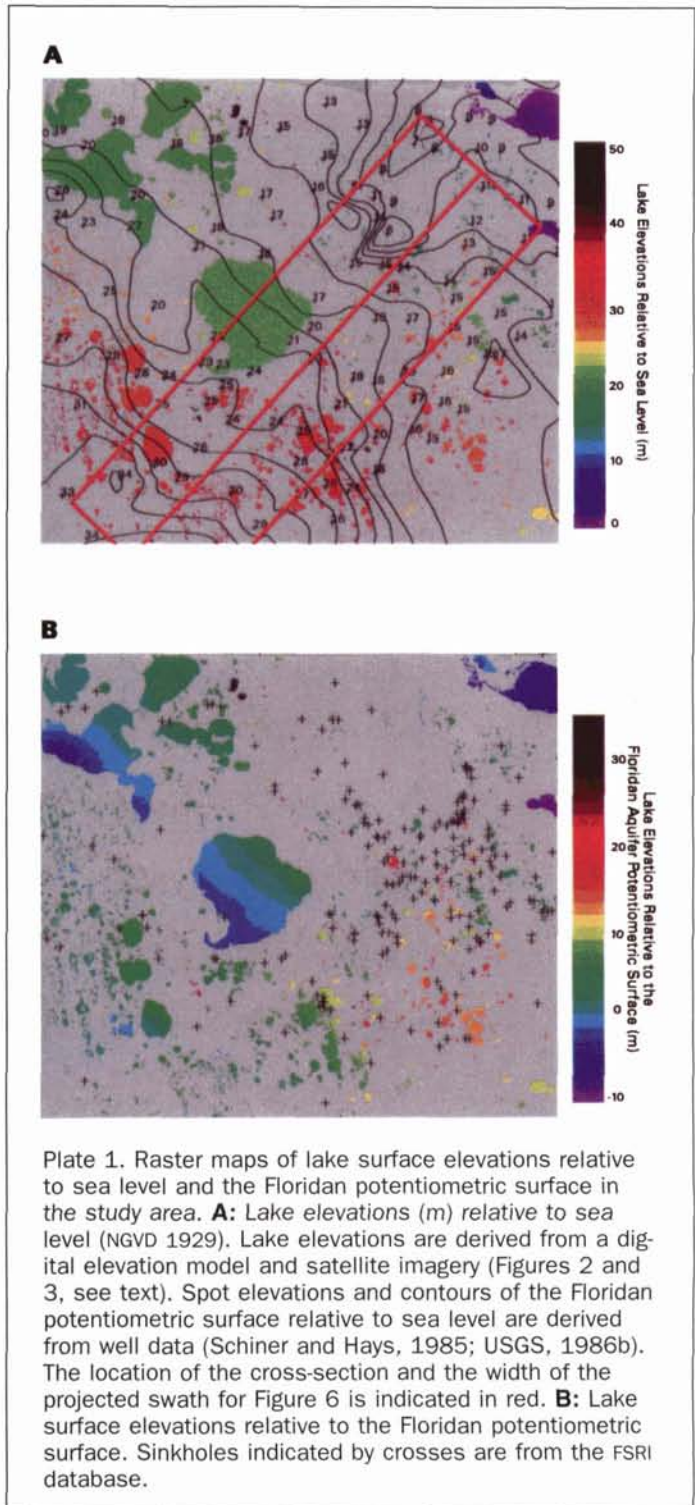
### Aquifer Head Difference and Sinkhole Occurrence

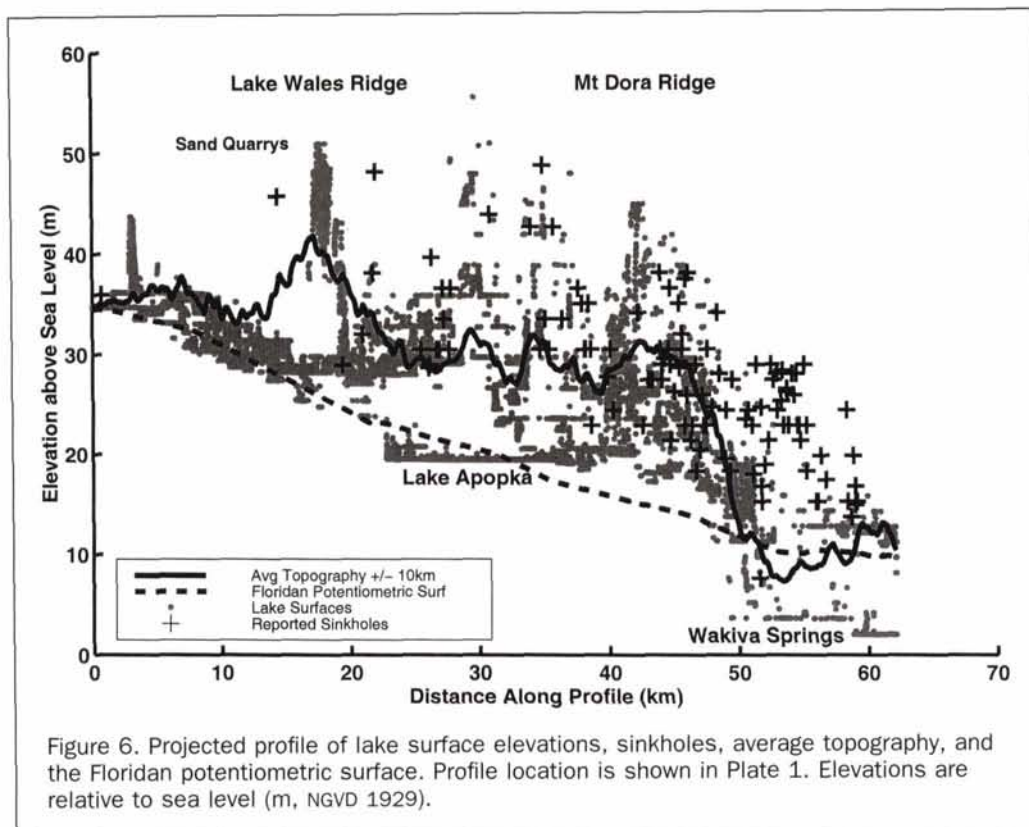
A qualitative examination of the spatial relationships between hydrostatic head difference and reported sinkhole occurrence reveals that lakes at elevations greater than 10 m above the level of the Floridan are spatially associated with the locations of reported sinkholes (Plate 1B). Conversely, regions with few sinkholes tend to have a low head difference. This correlation is not perfect; the areas of highest sinkhole density are not always coincident with the areas of highest head difference. In most cases, however, sinkholes are in close proximity to lakes with high head difference.

A southwest to northeast trending profile across the study area highlights the relationships between lake surface elevations, the potentiometric surface, and the locations of reported sinkholes (Plate 1A and Figure 6). This profile includes all lake grid cells and reported sinkholes within a 20-km-wide swath and the average level of both the surface topography and the potentiometric surface across the swath. In the southwest part of the profile, lake levels are tightly clustered at elevations between 0 and 5 m above the potentiometric surface, and relatively few sinkholes are observed. Sinkholes occur much more frequently in the central and

northeastern portions of the profile. In these sections of the profile, lakes tend to occur at higher elevations above the potentiometric surface and are much more widely dispersed in elevation. This suggests that both head difference and lateral changes in head difference are important influences in sinkhole occurrence.

These qualitative visual observations of spatial coincidence provide the basis of a hypothesis that can be tested quantitatively: Are areas of high sinkhole occurrence spatially associated with areas of high head difference? Quantitative testing of this interpretation requires the comparison of the





spatial co-occurrence of sinkholes, represented as points, with lakes, represented as irregular polygons. Several methods of comparing point distributions do exist (Upton and Fingleton, 1985). It is usually simpler, however, to transform the point distributions to continuous raster layers and then compare the layers on a pixel-by-pixel basis (Figure 5). Cross-area tabulation is then used to quantify spatial associations between maps with summary statistics (Bonham-Carter, 1994).

The map of lake elevations relative to the potentiometric surface (Plate 1B) is a discretely sampled estimate of a continuous head difference surface. Therefore, it is appropriate to reconstruct this surface by interpolation. Head difference values for each lake pixel are used to construct a TIN surface model. This TIN is then linearly interpolated onto a 30-m-resolution grid. The resulting surface is shown in Figure 7A. Because the water table will generally be higher than a line connecting adjacent water bodies, this model should be viewed as a lower bound of the head difference potential within the study area.

The next step involves producing a continuous surface from the reported sinkhole locations. Two potential approaches exist. The first approach is to construct a sinkhole density map by applying a moving average kernel to the map shown in Plate 1B. The problem with this approach is that the moving average acts as a low-pass filter, reducing the spatial detail of the surface. In addition, the result is extremely dependent on kernel size. An alternative to a density map is to construct a map of sinkhole proximity. First, a regular 30-m grid is superimposed over the study area. Then, for each grid cell, the Euclidean distance from the grid cell center to each sinkhole location within the database is calculated. The minimum distance value is then assigned to that grid cell and the process is repeated for the next grid cell. In essence, this is a buffering operation between each cell in the raster grid and the nearest sinkhole point. The key to this

operation is that it avoids the bias inherent in a sinkhole density calculation; the resultant map is independent of grid cell size, and regriding-induced errors are avoided.

Quantized versions of the head difference and distance to nearest sinkhole grids are shown in Figure 7. An inspection of Figure 7A shows that the areas of highest head difference lie in a northwest trending swath to the east of Lake Apopka and in a diffuse cluster in the southeast corner of the study area. Inspection of Figure 7B reveals that there is a relatively high density of sinkholes in the eastern side of the study area. There is a large and semicontinuous region in which inter-sinkhole distance is less than 2 km. In contrast, in the western part of the study area, there are a number of discrete regions in which the inter-sinkhole distance is quite high. The maximum inter-sinkhole value reported here is approximately 12 km. Only a small fraction of the study area has inter-sinkhole distance values greater than 10 km.

The correlation between two continuous variables is often measured by a correlation coefficient such as Pearson's *r*. For spatial data, global correlations between mapped variables are usually not very great, and correlations often appear locally only under a given set of conditions (Bonham-Carter, 1994). A more illuminating method is to quantize the variables into a finite number of discrete classes and then compare the degree of overlap between given classes by means of a cross-area tabulation.

First, the head difference grid is quantized into 2.5-m head-difference horizontal slabs or "slices." Similarly, the sinkhole proximity grid is quantized into 1-km inter-sinkhole distance "slices." The study area contains a number of large lakes within which sinkholes presumably would not be observed or reported. In order to avoid the possible bias due to under reporting of sinkholes which occur within these lakes, all pixels covered by water bodies are assigned a value of null.

Following Bonham-Carter (1994), a contingency table

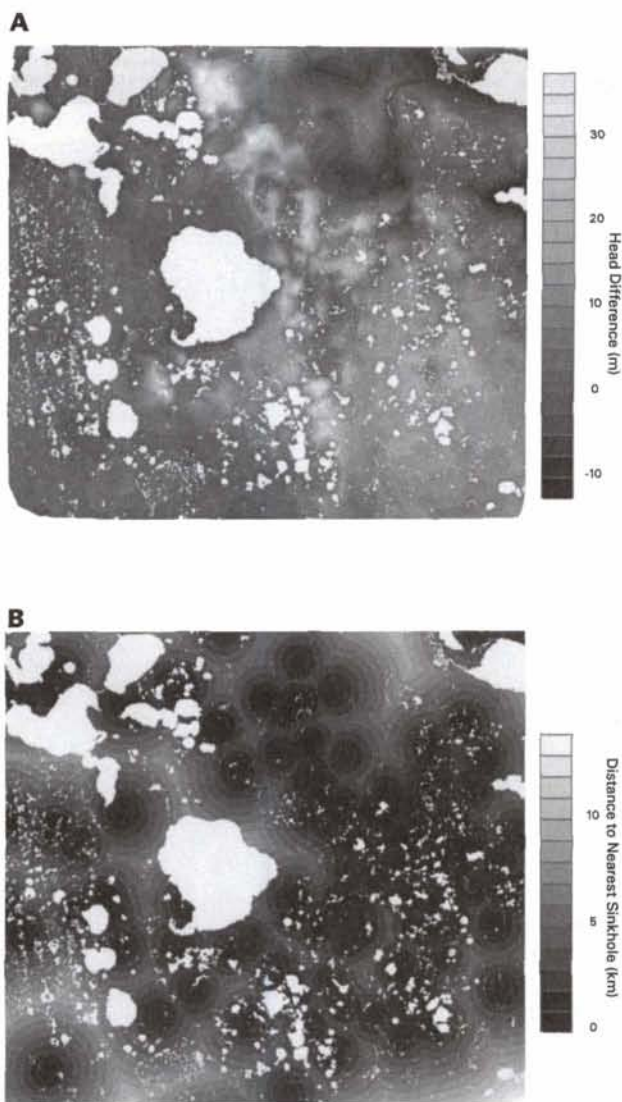


Figure 7. Head difference model and distance-to-nearest-sinkhole map for the study area. Horizontal resolution of grids are 30 m. **A:** Head difference model interpolated from map of lake elevations relative to the Floridan aquifer potentiometric surface (Plate 1B). The grid values quantized into 2.5-m-high slices. Lakes are shown in white. **B:** Map of distance to the nearest sinkhole. Map is generated by application of buffer zones to sinkholes shown in Figure 1 and Plate 1B. Map is quantized into 1-km-wide slices.

(Table 2) is constructed where total areas of each unique combination of head difference and distance to nearest sinkhole are tabulated. This table is in essence a two-dimensional histogram with elements  $T_{ij}$ , where  $i$  ranges from 1 to 18, the total number of discrete head difference intervals, and  $j$  ranges from 1 to 12, the total number of distance-to-nearest-sinkhole intervals. Each row of the table corresponds to a discrete head-difference interval bin and presents a one-dimensional histogram of the corresponding distance-to-nearest-sinkhole values for that bin. The summary row containing the marginal totals,  $T_{j\cdot}$ , is the distribution histogram of distance-to-nearest-sinkhole values by area for the entire study area. Each column of the table, corresponds to a discrete distance-to-nearest-sinkhole interval and presents a

one-dimensional histogram of the head difference distribution. The summary column,  $T_{i\cdot}$ , is the distribution histogram for head differences for the entire study area. The total area of study (minus lakes),  $T_{\cdot\cdot}$ , is obtained by summing over both rows and columns.

The cross-area tabulation and distribution histograms are shown graphically in Figure 8. The bulk of the study area is represented by a broad maximum located at head differences of between 0 and 5 m, spanning an interval of distance-to-nearest-sinkhole values from 0 to 8 km (Figure 8A). A smaller yet distinct maximum is centered at a head difference of approximately 12 m, which is located generally at distance-to-nearest-sinkhole values of less than 4 m. This secondary maxima is more clearly indicated in the head difference distribution histogram (Figure 8B). This histogram appears bimodal, with the peaks corresponding to area populations centered near 0 and 10 m, respectively.

The areal distribution histogram of distance to nearest sinkhole within the study area is indicated in Figure 8C. The distance-to-nearest-sinkhole histogram (Figure 8C) is a skewed unimodal distribution which peaks between 1 and 2 km. For comparison, the expected distribution for an independent and randomly located (e.g., Poisson) population of 226 sinkholes within the study area is shown in the solid line. This comparison reveals that the observed distribution has larger inter-sinkhole distances than would be expected for a random distribution. This behavior implies a non-randomness or clustering within the observed spatial distribution.

One possible explanation for the long tail of the observed distribution is that sinkhole occurrence is suppressed in regions of low head difference and is enhanced in areas of high head difference. In order to explore this assertion, the area tabulation is split into two parts at the 5-m threshold and replotted into two separate curves (Figure 8D). This subdivision is justified on the basis of the bimodal distributions suggested in Figures 8A and 8B. The anomalous areas of large inter-sinkhole distance are mainly associated with areas with head differences less than 5 m.

Another relevant way to evaluate the association between the maps shown in Figures 7A and 7B is to compare the observed contingency table with one expected from independent phenomena. The marginal totals  $T_{i\cdot}$  and  $T_{\cdot j}$  correspond to the frequency distributions of head difference and distance to nearest sinkhole, respectively. If these two phenomena are statistically independent, then the expected cross distribution  $T_{ij}^*$ , is given by the product of the marginal totals divided by the grand total (Bonham-Carter, 1994): i.e.,

$$T_{ij}^* = \frac{T_{i\cdot} T_{\cdot j}}{T_{\cdot\cdot}}$$

A comparison of the observed and expected cross distributions is shown in Figure 9. For regions of inter-sinkhole distances greater than 4 km, the observed cross distribution (Figure 9A) shows greater areas at low head differences ( $\Delta h < 5$  m) and lesser areas at high head differences ( $\Delta h > 5$  m) than the expected cross distribution (Figure 9B). Subtraction of the expected from the observed distribution yields the area residual shown in Figure 9C. The area residual shows the pattern and degree of spatial association between head difference and sinkhole proximity. Regions 2 km or less from the nearest sinkhole show a strong positive association to head differences between 5 and 15 m and a negative association with head differences between 0 and 2.5 m. In contrast, areas with inter-sinkhole distances between 4 and 8 km show a strong positive association with head differences between 0 and 2.5 m and a negative association with head differences between 5 and 15 m. In other words, in areas of low

TABLE 2. AREA CROSS-TABULATION OF SLICED HEAD DIFFERENCE AND DISTANCE-TO-NEAREST-SINKHOLE GRIDS. AREA UNITS ARE IN KM<sup>2</sup>. THE FAR RIGHT COLUMN AND THE BOTTOM ROW REPRESENT THE MARGINAL TOTALS  $T_i$  AND  $T_j$ , RESPECTIVELY. THE GRAND TOTAL,  $T_{..}$ , IS SUMMED OVER BOTH ROWS AND COLUMNS AND EQUALS THE TOTAL AREA OF THE STUDY (MINUS LAKES).

Head Difference (m)	Distance to Nearest Sinkhole (km)												$T_i$	
	0	1	2	3	4	5	6	7	8	9	10	11		
>32.5	0	0	1	3	3	0	0	0	0	0	0	0	0	7
30.0 to 32.5	0	1	3	2	1	0	0	0	0	0	0	0	0	7
27.5 to 30.0	0	2	4	3	1	0	0	0	0	0	0	0	0	7
25.0 to 27.5	0	4	4	2	1	0	0	0	0	0	0	0	0	11
22.5 to 25.0	2	5	5	3	1	0	0	0	0	0	0	0	0	16
20.0 to 22.5	3	8	8	4	2	0	0	0	0	0	0	0	0	24
17.5 to 20.0	7	11	10	7	3	1	0	0	0	0	0	0	0	38
15.0 to 17.5	22	23	16	10	6	1	0	0	0	0	0	0	0	79
12.5 to 15.0	48	67	63	41	19	6	2	2	1	0	0	0	0	247
10.0 to 12.5	62	67	57	44	23	15	13	8	6	2	1	2	2	299
7.5 to 10.0	55	58	38	31	17	9	7	11	7	5	4	3	3	244
5.0 to 7.5	57	79	63	40	25	17	9	6	5	3	1	0	0	304
2.5 to 5.0	69	107	106	83	70	49	44	25	11	4	0	0	0	567
0.0 to 2.5	49	111	123	109	90	79	62	41	11	3	2	0	0	679
-2.5 to 0.0	13	29	31	24	28	23	22	15	9	2	0	0	0	195
-5.0 to -2.5	5	11	13	12	13	8	7	5	4	2	0	0	0	82
-7.5 to -5.0	0	2	6	6	4	5	5	4	0	0	0	0	0	34
-10.0 to -7.5	0	0	1	2	3	4	1	0	0	0	0	0	0	12
$T_j$	392	584	551	427	308	218	172	114	55	20	7	5	5	2853
														$T_{..}$

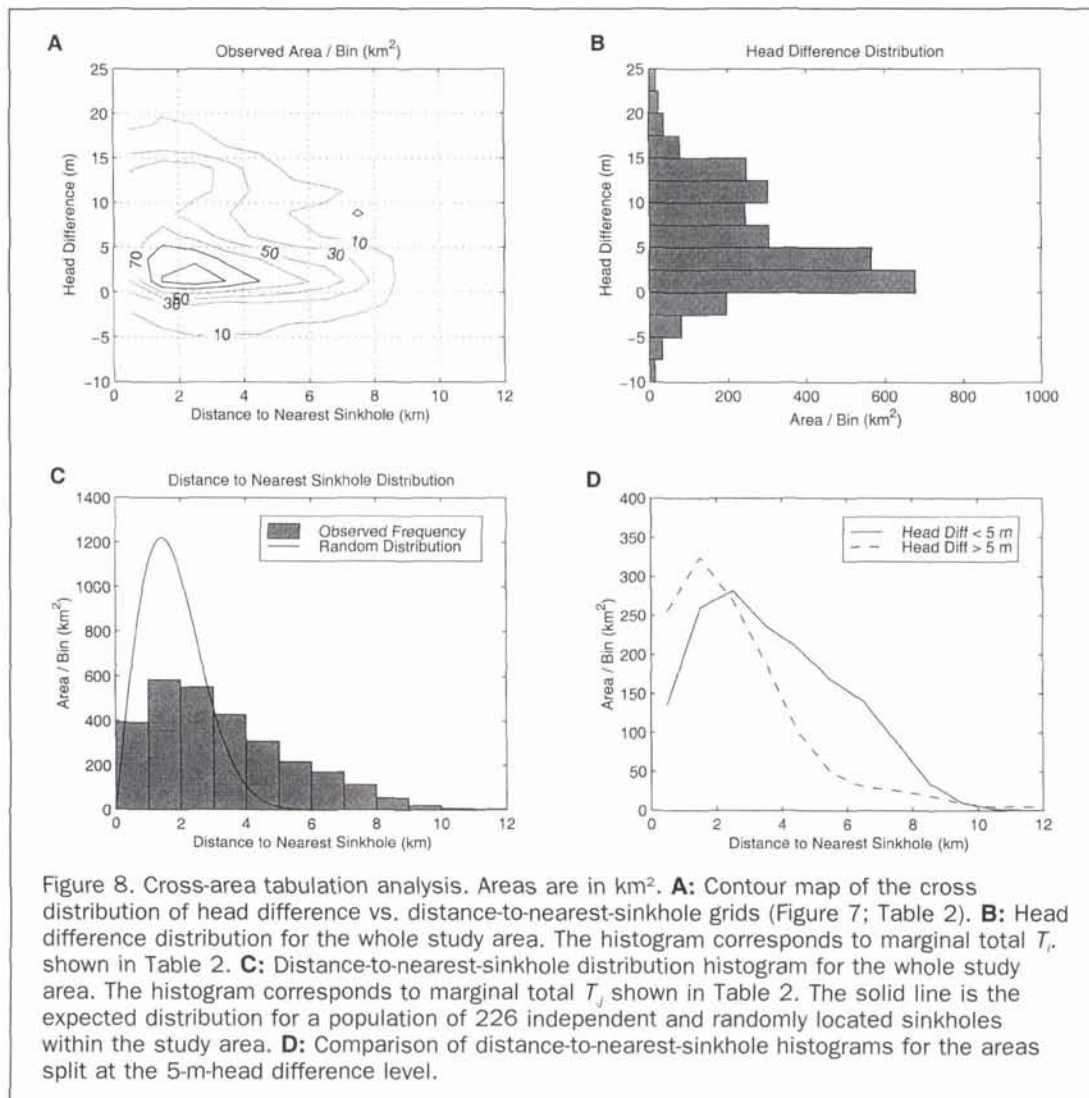


Figure 8. Cross-area tabulation analysis. Areas are in km<sup>2</sup>. **A:** Contour map of the cross distribution of head difference vs. distance-to-nearest-sinkhole grids (Figure 7; Table 2). **B:** Head difference distribution for the whole study area. The histogram corresponds to marginal total  $T_i$  shown in Table 2. **C:** Distance-to-nearest-sinkhole distribution histogram for the whole study area. The histogram corresponds to marginal total  $T_j$  shown in Table 2. The solid line is the expected distribution for a population of 226 independent and randomly located sinkholes within the study area. **D:** Comparison of distance-to-nearest-sinkhole histograms for the areas split at the 5-m-head difference level.



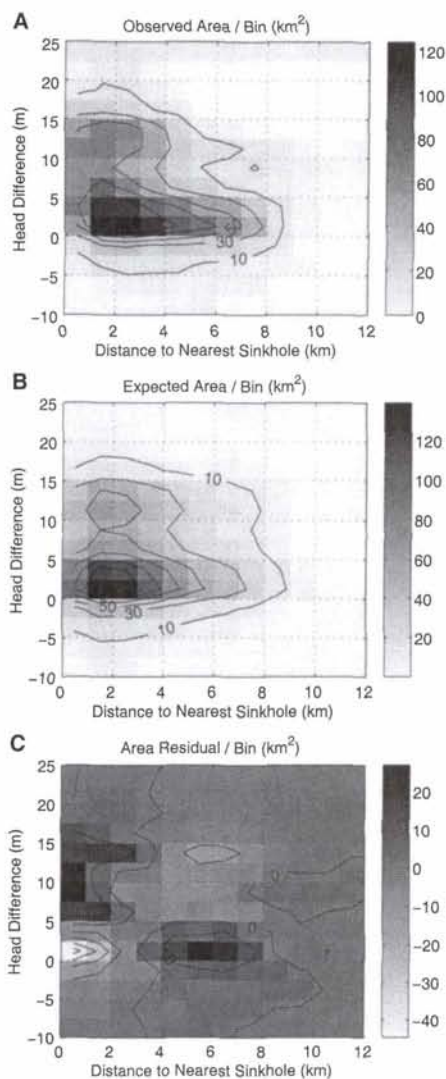


Figure 9. Cross-area residual analysis. **A:** Observed cross distribution of head difference and distance-to-nearest-sinkhole grids (Figure 7; Table 2). **B:** Expected cross distribution assuming independence of head difference and distance to nearest sinkhole. **C:** Residual (observed - expected) cross distribution. Dark areas show positive associations between head difference and distance-to-nearest sinkhole. Light areas show negative associations.

head difference, sinkholes are less frequent and farther apart than expected. Conversely, in areas of high head difference, sinkholes are more common and more closely spaced than one would expect.

### Discussion

The association of sinkhole proximity to head differences between the surficial and Floridan aquifers demonstrates the importance of hydrostatic loads in sinkhole hazard. In particular, sinkhole formation appears to be retarded where head difference is low. This result is consistent with previously reported temporal associations between aquifer drawdown

and sinkhole formation (Sinclair, 1982; Metcalfe and Hall, 1984; Newton, 1984; Sinclair *et al.*, 1985; Sinclair and Stewart, 1985; Wilson and Beck, 1992). The highest sinkhole density is not always coincident with the highest head differences (Plate 1 and Figure 7). Instead, the relationship appears to be one of sinkhole *proximity* to regions of high head difference and to regions of rapid horizontal change in head difference (see Figures 6 and 7).

Head difference is related to a complex set of factors and reflects the dynamic equilibrium between the surficial and Floridan aquifer systems. A limiting factor is the height of the land surface relative to the potentiometric surface. High head differences cannot exist in lowlands where the ground lies near or below the potentiometric surface. The Lake Wales and Mt. Dora ridges form the most prominent physiographic features of the study area. Both ridges are underlain by similar thicknesses of clastic cover (Lichtler *et al.*, 1968). Their average heights both lie approximately 15 m above the potentiometric surface (Figure 6). Only the Mt. Dora ridge is associated with head differences high enough to drive sinkhole formation (compare Figures 1 and 7B). Apparently, elevated regions of thick surficial cover are not always associated with sinkhole formation. Instead, head difference appears to be the key factor.

Wilson and Beck (1992) observed that 85 percent of the new sinkholes near Orlando, Florida occurred within the high groundwater recharge areas defined by Lichtler *et al.* (1968). Within their study area, these high recharge areas correspond to the Mt. Dora and Orlando ridges. Their study area was confined to Orange and Seminole Counties and thus did not include the Lake Wales ridge to the west. Their reported association of sinkhole formation with recharge areas overlooked the variability of head difference between recharge areas because the eastern boundary of their study area happened to exclude the Lake Wales ridge. Our decision to include the Lake Wales ridge was driven by the results of synoptic regional terrain analysis using remote sensing and GIS techniques; the results demonstrate the value of these techniques to further sinkhole studies.

We suggest that mapped areas of high head difference may be a useful predictor of sinkhole hazard. The Orlando metropolitan area derives virtually all of its municipal, industrial, and agricultural water supplies from the Floridan aquifer and this water use has resulted in declines in the potentiometric surface of as much as 6 m since the 1930s (Murray and Halford, 1996). The regions of greatest decline are coincident with our mapped areas of high head difference. Continued groundwater withdrawals will likely increase sinkhole hazard in the future.

### Conclusions

GIS and GIS-derived datasets are useful tools in evaluating regional factors associated with sinkhole hazard in central Florida. These methods show that sinkholes within the study area are not distributed randomly but instead appear to be clustered in space. In general, they are found in close proximity to lakes whose surfaces are perched at elevations significantly above the potentiometric surface of the Floridan aquifer. These lakes delineate regions where the head difference between the surficial and the Floridan aquifer systems is high. Regions 2 km or less from the nearest sinkhole show a strong positive association to head differences between 5 and 15 m and a negative association with head differences between 0 and 2.5 m. In contrast, areas with inter-sinkhole distances between 4 and 8 km show a strong positive association with head differences between 0 and 2.5 m and a negative association with head differences between 5 and 15 m. In other words, in areas of low head difference, sinkholes are less frequent and farther apart than expected. Conversely, in

areas of high head difference, sinkholes are more common and more closely spaced than one would expect. This association of sinkhole proximity to head differences demonstrates the importance of hydrostatic loads in sinkhole hazard.

### Acknowledgment

The authors wish to acknowledge helpful suggestions given by W. Wilson, G. Draper, and F. Maurrasse. S. Spenser and W. Wilson provided versions of the sinkhole database. B. Branch provided computer system support at Florida International University. This study was partially supported by NASA Grant # NAG 5-307.

### References

- Benson, R.C., and L.J. La Fountain, 1984. Evaluation of subsidence or collapse potential due to subsurface cavities, *Proceedings of the First Multidisciplinary Conference on Sinkholes* (B.F. Beck, editor), A.A. Balkema, Rotterdam, pp. 201-216.
- Bonham-Carter, G.F., 1994. *Geographic Information Systems for Geoscientists: Modeling with GIS*, Pergamon Press, [place of publication], 398 p.
- Boniol, D., M. Williams, and D. Munch, 1993. *Mapping Recharge to the Floridan Aquifer Using a Geographic Information System*, Technical Publication SJ93-5, Saint Johns River Water Management District, Palatka, Florida, 41 p.
- Florida Geological Survey, 1986. *Hydrogeologic Units of Florida*, Florida Geological Survey Special Publication No. 28, Tallahassee, Florida, 9 p.
- Jammal and Associates, Inc., 1982. *The Winter Park Sinkhole, Geotechnical Engineering Report*, submitted to the city of Winter Park, Florida by Jammal and Associates, Inc., Winter Park, Florida, 274 p.
- Lane, E., 1986. *Karst in Florida*, Florida Geological Survey Special Report No. 29, Tallahassee, Florida, 100 p.
- Lichtler, W., W. Anderson, and B. Joyner, 1968. *Water Resources of Orange County, Florida*, Florida Geological Survey Report of Investigations No. 50, Tallahassee, Florida, 150 p.
- Lichtler, W.F., G.H. Hughes, and F.L. Pfischner, 1976. *Hydrologic Relations between Lakes and Aquifers in a Recharge Area Near Orlando, Florida*, U.S. Geological Survey Water Resources Investigation 76-65, Tallahassee, Florida, 54 p.
- Metcalfe, S.J., and L.E. Hall, 1984. Sinkhole Collapse Induced by Groundwater Pumpage from Freeze Protection Irrigation Near Dover, Florida, January, 1977, *Sinkholes: Their Geology, Engineering and Environmental Impact* (B.F. Beck, editor), A.A. Balkema Pub., Rotterdam, pp. 29-34.
- Miller, J.A., 1986. *Hydrologic Framework of the Floridan Aquifer System in Florida and Parts of Georgia, Alabama, and South Carolina*, U.S. Geological Survey Professional Paper No. 1403-B, Washington, D.C., 91 p.
- , 1997. Hydrogeology of Florida, *The Geology of Florida* (A. Randazzo and D. Jones, editors), University Press of Florida, Gainesville, Florida, pp. 69-88.
- Monroe, W., 1970. *A Glossary of Karst Terminology*, U.S. Geological Survey Water Supply Paper No. 1899-K, Reston, Virginia, 26 p.
- Motz, L.H., 1998. Vertical Leakage and Vertically Averaged Vertical Conductance for Karst Lakes in Florida, *Water Resources Research*, 34:159-167.
- Murray, L.C., Jr., and K.J. Halford, 1996. *Hydrogeologic Conditions and Simulation of Groundwater Flow in the Greater Orlando Metropolitan Area, East-Central Florida*, U.S. Geological Survey Water Resources Investigations Report No. 96-4181, Tallahassee, Florida, 100 p.
- Newton, J.G., 1984. Review of Induced Sinkhole Development, *Sinkholes: Their Geology, Engineering and Environmental Impact* (B.F. Beck, editor), A.A. Balkema Pub., Rotterdam, pp. 3-10.
- , 1987. *Development of Sinkholes Resulting from Man's Activities in the Eastern United States*, U.S. Geological Survey Circular No. 96854, Reston, Virginia, 54 p.
- Schmidt, W., and T.M. Scott, 1984. Florida Karst — Its Relationship to Geologic Structure and Stratigraphy, *Sinkholes: Their Geology, Engineering and Environmental Impact* (B.F. Beck, editor), A. A. Balkema Pub., Rotterdam, pp. 11-16.
- Sinclair, W., 1982. *Sinkhole Development Resulting from Groundwater Withdrawal in the Tampa Area, Florida*, U.S. Geological Survey Water Resources Investigations Report No. 81-50, Tallahassee, Florida, 19 p.
- Sinclair, W.C., and J.W. Stewart, 1985. *Sinkhole Type, Development, and Distribution in Florida*, Florida Geological Survey Map Series No. 110, Tallahassee, Florida, 1 p.
- Sinclair, W., J. Stewart, R. Knutilla, A. Gilboy, and R. Miller, 1985. *Types, Features, and Occurrence of Sinkholes in the Karst of West-Central Florida*, U.S. Geological Survey Water Resources Investigations Report No. 85-4126, Tallahassee, Florida, 81 p.
- Spencer, S.M., and E. Lane, 1995. *Florida Sinkhole Index*, Florida Geological Survey Open File Report No. 58, Tallahassee, Florida, 18 p.
- Sweeting, M., 1973. *Karst Land Forms*, Columbia University Press, New York, 862 p.
- Upchurch, S., and A. Randazzo, 1997. Environmental Geology of Florida, *The Geology of Florida* (A. Randazzo and D. Jones, editors), University Press of Florida, Gainesville, Florida, pp. 217-250.
- USGS, 1986a. *Water Resources Data Florida, Water Year 1986, Volume 1A: Northeast Florida Surface Water*, U.S. Geological Survey Water-Data Report No. FL86-1A, Tallahassee, Florida, 242 p.
- , 1986b. *Water Resources Data Florida, Water Year 1986, Volume 1B: Northeast Florida Ground Water*, U.S. Geological Survey Water-Data Report No. FL86-1B, Tallahassee, Florida, 214 p.
- White, W.A., 1970. *The Geomorphology of the Florida Peninsula*, Florida Bureau of Geology Bulletin No. 51, Tallahassee, Florida, 164 p.
- White, W.B., 1988. *Geomorphology and Hydrology of Karst Terrains*, [publisher], New York, xxx p.
- Wilson, W., and B. Beck, 1988. Evaluating Sinkhole Hazards in Mantled Karst Terrain, *Geotechnical Aspects of Karst Terrains Special Volume*, American Society of Civil Engineers, New York, N.Y., pp. 1-24.
- , 1992. Hydrogeologic Factors Affecting New Sinkhole Development in the Orlando Area, Florida, *Ground Water*, 30:918-930.
- Wilson, W., and E. Shock, 1996. *New Sinkhole Data Spreadsheet Manual: A Description of Quantitative Methods for Modeling New Sinkhole Frequency, Size Distribution, Probability and Risk, Based on Actuarial Statistical Analysis of the New Sinkhole Data Spreadsheet*, unpublished report, Subsurface Evaluations, Inc., Winter Springs, Florida, 31 p.

(Received 29 October 1998; revised and accepted 19 November 1998)